Environmental Science
Water Research & Technology

ROYAL SOCIETY OF CHEMISTRY

PAPER

View Article Online
View Journal | View Issue

Check for updates

Cite this: *Environ. Sci.: Water Res. Technol.*, 2025, **11**, 3001

Tyre wear particles in a highway stormwater system during rain: quantification by automatic sampling and pyrolysis-GC/MS, and correlations with metals and solids

Elly Lucia Gaggini, *[a] Ekaterina Sokolova, [b] Elisabeth Støhle Rødland,[c] Ann-Margret Strömvall, [a] Yvonne Andersson-Sköld[de] and Mia Bondelind [a]

Received 14th July 2025,
Accepted 2nd October 2025

DOI: 10.1039/d5ew00656b

rsc.li/es-water

Tyre wear particles (TWP) are a major microplastic pollutant in road runoff, yet their transport dynamics in stormwater remain poorly understood. This study investigates the abundance and dynamic behaviour of TWP during rain events in a highway stormwater system between March and May 2023. Road runoff was collected from gully pots and stormwater wells using automatic samplers during rain events and analysed for TWP, elements, total suspended solids (TSS), volatile suspended solids (VSS) and turbidity. Quantification of TWP was performed using pyrolysis-gas chromatography/mass spectrometry for size fractions of 1.6–20 μm and 1.6–500 μm. Results show that TWP concentrations ranged from 9–170 mg L^{-1} for the larger size fraction, and 8–150 mg L^{-1} for the fine size fraction, with higher concentrations at the beginning of the rain event, suggesting a first-flush effect or sediment resuspension. The majority, 87 ± 13% on average, of TWP were quantified in the fine size fraction (1.6–20 μm). The findings indicate that TWP are mobilised from road surfaces and resuspend from gully pot sediments, thus resulting in low retention of TWP in the stormwater system. Additionally, high concentrations of metals, such as Cr, Cu, and Zn, were measured. Strong correlations were observed between TWP, TSS, VSS, and metals, suggesting shared transport pathways. These findings contribute to understanding the dynamic TWP transport behaviour during rain events, supporting better design of stormwater treatment systems targeting this emerging contaminant.

Water impact

Tyre wear particles (TWP) are an understudied contaminant in stormwater. Using automatic sequential sampling, we showed that TWP concentrations peaked at rainfall onset, with many particles in the fine size fraction (<20 μm), a fraction rarely assessed before. TWP correlated with TSS, VSS, and some metals, indicating co-transport. Common Swedish gully pots provided little retention, especially for TWP in the fine size fraction, highlighting the limited effectiveness of sedimentation-based systems. This study underscores the need for treatment solutions designed for high flows and small particles and informs stormwater management targeting TWP.

Introduction

Microplastics have received growing attention in recent years due to their ubiquitous presence in stormwater[1,2] and high emissions. Tyre wear particles (TWP), which may also be included in the definition of microplastics,[3] have been highlighted as a major source of microplastics.[4] TWP emissions are estimated at approximately 6 000 000 tonnes per year globally,[4] with 11 000–12 000 tonnes per year estimated for Sweden alone,[5] though these figures remain uncertain due to lack of measured emission factors.[6] Concerns regarding TWP emissions stem, aside from their magnitude, also from the reported toxic effects of TWP leachates identified in laboratory studies.[7–11] These issues are likely to persist even for eco-friendly tyres, as they have a similar composition of metals and organic compounds to ordinary tyres.[12]

Quantifying TWP in environmental matrices presents significant analytical challenges, particularly for finer particle

[a] *Water Environment Technology, Department of Architecture and Civil Engineering, Chalmers University of Technology, SE-412 96 Gothenburg, Sweden. E-mail: elly.gaggini@chalmers.se*
[b] *Program for Air, Water and Landscape Sciences, Hydrology, Department of Earth Sciences, Uppsala University, SE-752 36 Uppsala, Sweden*
[c] *Norwegian Institute for Water Research, Økernveien 94, NO-0579 Oslo, Norway*
[d] *Swedish National Road and Transport Research Institute (VTI), Box 8072, SE-402 78 Gothenburg, Sweden*
[e] *Division of Geology and Geotechnics, Department of Architecture and Civil Engineering, Chalmers University of Technology, SE-412 96 Gothenburg, Sweden*

Open Access Article. Published on 22 October 2025. Downloaded on 4/9/2026 1:40:24 PM.
This article is licensed under a Creative Commons Attribution 3.0 Unported Licence.

Open Access Article. Published on 22 October 2025. Downloaded on 4/9/2026 1:40:24 PM. This article is licensed under a Creative Commons Attribution 3.0 Unported Licence.

sizes.[13] These difficulties also arise from the lack of standardised analytical methods and comprehensive data on tyre compositions.[14] Pyrolysis-gas chromatography/mass spectrometry (Pyr-GC/MS) methodologies based on different pyrolysis marker compounds have been used for TWP quantification in environmental matrices.[15–28] However, considerable variability in the quantification of rubber content of tyres has been reported for pyrolysis markers 4-vinylcyclohexene (VCH; the proposed marker in the ISO specifications), SB hybrid dimer and SBB hybrid trimer,[16] whereas the use of a combination of multiple markers was found to yield lower variability for Norwegian tyres.[19]

Stormwater is a major pathway for TWP to be mobilised from the road surface during precipitation and to be transported to roadside soils and water systems. High mass concentrations have been quantified in stormwater,[17,29] and studies suggest that TWP were the prevalent microplastic in urban stormwater,[30] and both rubber and bitumen particles occurred in high concentrations in stormwater from a highway.[31] However, few studies have investigated the transport of microplastics during rain events.[32–34] The dynamic behaviour of TWP in runoff during rainfall and the processes of how TWP are transported during rain events remain largely unstudied, and a clearer understanding of these processes can inform the design and improvement of stormwater treatment solutions tailored to remedy this emerging contaminant.

Some previous studies on runoff, tunnel wash water and snow samples have shown strong correlations between total suspended solids (TSS) and TWP concentrations;[17,18,22,35] this could indicate that TWP behave as another road particulate material during rainfall, but due to the limited number of studies investigating this, it is still uncertain.

The aim of this study was to investigate the abundance and dynamic behaviour of TWP through a stormwater system during rain events through automatic time-proportional sampling and pyrolysis-gas chromatography/mass spectrometry (Pyr-GC/MS) analysis with multiple markers. The objectives were to:

- Measure the event mean concentrations (EMCs) of TWP emitted through a highway stormwater system during two rain events.
- Assess the loading distribution of TWP concentrations during two rain events in consecutive gully pots and wells of a highway stormwater system.
- Analyse the proportion of TWP in the fine particle size fraction of 1.6–20 μm during rain events for selected samples.
- Characterise the behaviour of TWP through comparison with other stormwater related parameters (total suspended solids (TSS), volatile suspended solids (VSS), and turbidity) and pollutants (total metals) in the same stormwater system.

Materials and methods

Study area

The sampling campaign was carried out between 2023-03-28 and 2023-05-30 at the stormwater system of Testsite E18 by highway E18, a road research facility of the Swedish Transportation Administration.[36] The test site is located between Västerås and Enköping (59°38′01.9″N 16°51′18.7″E), in an open rural area (Fig. 1). This section of highway E18 was built in 2010 and has about 12 000 AADT, 830 of which are heavy-duty vehicles.[37] The highway has two lanes in each direction, and the speed limit is 120 km h^{-1}, and the road pavement cover consists of stone mastic asphalt with residues of the old pavement combined using warm-remixing in 2021. The old pavement also included polymer-modified butadiene (PMB). Measuring equipment on-site (Vaisala RWS200) monitors weather and traffic data every 10 minutes.

A 100 m long stretch of the highway (yellow area in Fig. 1) with a surface area of approximately 600 m^2 is sealed off through a kerb, directing the runoff from the first lane into two gully pots (GP1 and GP2). The gully pots are serially connected, and GP2 discharges the runoff into a collecting well equipped with a Thomson weir (WA, SI Fig. S3), connected to collecting well F, receiving the runoff from a larger area (for more details see Gaggini *et al.*[17]). Finally, the stormwater is discharged in a ditch adjacent to the highway, leading down to Lillån stream. The dimensions of the wells GP1, GP2 and WA can be found in SI Table S2.

Automatic time-proportional sampling

Three automatic time-proportional samplers were installed in the standing water volumes of the sand traps of two gully pots (location GP1 – sampler model ISCO 6712c, and location GP2 – model ISCO 6712) and of the well receiving water from the two gully pots (location WA – model ISCO 6712c). Two ISCO-samplers were equipped with 24 polyethylene bottles of volume 0.5 L (locations GP1 and WA), and one sampler with 24 polypropylene bottles of volume 1 L (location GP2). At all locations, the inlet hose was installed in the standing water volume of the wells. In the gully pots GP1 and GP2, a water level meter was installed in the water volume to trigger the sampler at a water level of 10 mm over the bottom of the outlet. In the well WA, sampling was triggered through a flowmeter installed *ca.* 20 cm into the outlet pipe from the well. The flow meter was set to trigger the sampler at a measured flow of 1.5 L. The samplers were programmed to take 1 L sample every 2.5 minutes when triggered. Out of 5 rain events sampled during the campaign, sampling at all three locations during the same rain event was only successful on 2023-04-29 and 2023-05-17, and therefore these rain events were selected for TWP analysis. The intensity over time of each rain event and the samples collected can be seen in SI 1.1. Samples were retrieved from Testsite E18 after 6 days and 1 day, respectively. All samples collected were re-bottled into glass bottles and stored in a fridge at a temperature of 4–8 °C.

Sample preparation and analyses

Procedure for quantification of TWP. The Pyr-GC/MS methodology for TWP quantification employed in this study was developed by Rødland *et al.*,[19] and has been applied by

 This journal is © The Royal Society of Chemistry 2025

Open Access Article. Published on 22 October 2025. Downloaded on 4/9/2026 1:40:24 PM.
This article is licensed under a Creative Commons Attribution 3.0 Unported Licence.

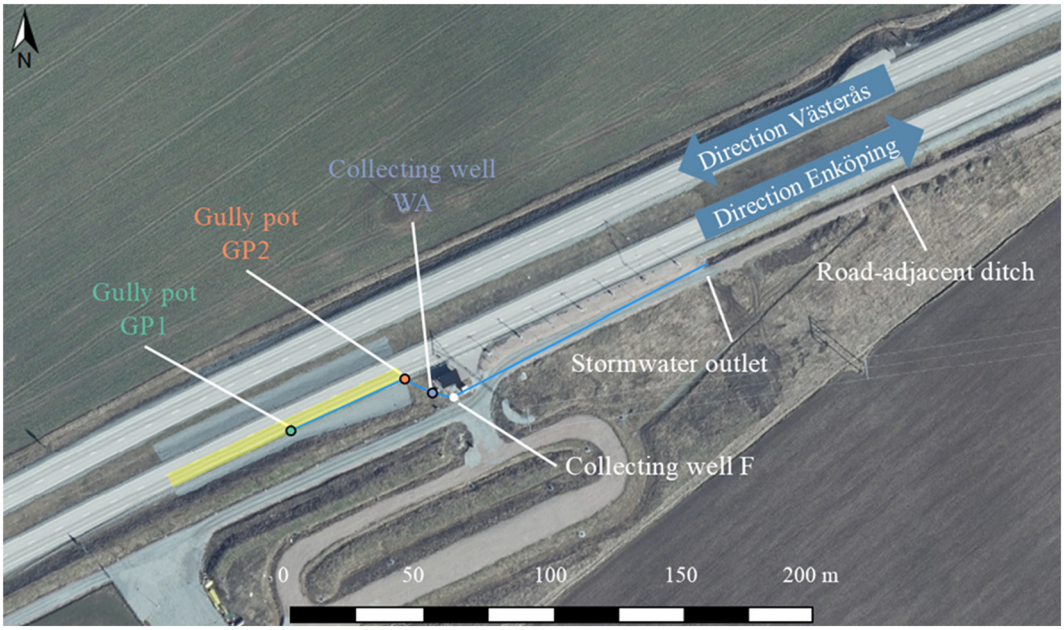

Fig. 1 Map of Testsite E18 with illustration of the stormwater system by the highway. Maps were retrieved and adapted from the Swedish Land Survey. The yellow area represents the catchment of the stormwater system, and blue lines indicate the stormwater path though pipes. Coloured and white circles represent wells.

several studies on water, sediment, snow, and soil samples.[15–22] An overview of the methodology is given in this section, whereas the details of the methodology can be found in the previous work and in SI 2.

The preparations of the samples for Pyr-GC/MS analyses of styrene–butadiene rubber and butadiene rubber (SBR + BR) were performed 6–8 months after sampling. Selected samples were analysed in two or three replicates (SI Table S9). Based on the TSS results (see the Procedures for total suspended solids, volatile suspended solids, turbidity and metal analyses section), the subsample volumes retrieved were adjusted to obtain less than 5 mg of dried mass on the filters to avoid SBR + BR levels over the detection limit, yielding volumes of 2–26 mL. Most of the water samples were retrieved from the shaken bottles directly, whereas the smallest volumes (<10 mL per bottle) were pipetted from a homogenised subsample for more precision. The retrieved subsamples were wet-sieved to remove particles >500 μm (VWR test sieve 3310 500 μm). All samples had a high particle content (TSS above 70 mg L^{-1}); therefore, the wet-sieved subsamples were transferred to 50 mL Falcon tubes and centrifuged (Labex Sigma 4-16, 3000 rpm min^{-1}, 10 min) for easier filtration. The supernatant was filtered first, followed by resuspension of the sedimented particles from the centrifugation with ultrapure water and ethanol onto the same filter.[18] The filtration set-up consisted of glass filtration equipment under vacuum and binder-free glass fibre filters (GF/A, Whatman, pore size 1.6 μm, diameter 25 mm). The filters were pre-treated in a muffle furnace at 550 °C. All dry filters were weighed before and after filtration. Based on the weight of the solid material (1.6–500 μm particles) and the original subsample volume before wet-sieving, TSS based on 25 mm filters was also calculated, referred to as the TSS 25 mm filter.

The outer circle (10 mm) of the filters around the filter cakes was removed, and the filters with filter cakes were rolled and put into pyrolysis cups for analysis. The samples were analysed for the total SBR + BR concentrations using Pyr-GC/MS with a marker combination of benzene, α-methylstyrene, ethylstyrene, and butadiene trimer (marker combination *a*, SI 2.1). The accuracy for this method was 85–151% in spiked environmental samples.[19] For samples with high benzene concentrations, the quantification of SBR + BR was performed without benzene as a marker (marker combination *b*, SI 2.1). The standard deviation across replicates was on average 9%, showing overall consistency of the methods and good homogenisation of the samples. Selected subsamples were also sieved through a VWR test sieve ISO 3310 20 μm in the wet-sieving step, to obtain the SBR + BR concentration in the fine fraction of 1.6–20 μm. The proportion of TWP in the fine fraction was assessed by dividing the SBR + BR concentration in the fine fraction with the SBR + BR concentration in the whole fraction of 1.6–500 μm. Residues of the old PMB-asphalt cover, which contains styrene–butadiene–styrene that would be identified as SBR + BR from tyres during analysis, are not expected to affect the results considerably due to the low amounts.[17] Analysis of blank samples of sampling equipment and laboratory pre-treatment showed low levels of contamination (SI 2.2). Details of equipment, analysis settings, detection limits, blanks and quality control, pyrolysis calibration and TWP calculation can be found in SI 2.

To account for the variability in SBR + BR content across different tyres (ranging from 115 to 682 μg mg^{-1} in Norwegian

Open Access Article. Published on 22 October 2025. Downloaded on 4/9/2026 1:40:24 PM. This article is licensed under a Creative Commons Attribution 3.0 Unported Licence.

reference tyres[19]), TWP concentrations were estimated using Monte Carlo simulations based on the reference tyre database from Rødland *et al.*,[19] rather than applying a single average value for SBR + BR content in tyres (SI 2.3). The 100 000 Monte Carlo simulations were based on the SBR + BR content in 31 reference tyres (from personal and heavy-duty vehicles), on the ratio of personal and heavy-duty vehicles at Testsite E18, and on a styrene conversion factor (SI 2.3 eqn (1)).

Procedures for total suspended solids, volatile suspended solids, turbidity and metal analyses. Total suspended solids and VSS analysis were performed after 5.5–6.5 months from sampling on samples from 2023-04-29 and 2023-05-17, and also from rainfalls collected on 2023-04-05, 2023-04-12 and 2023-04-23. TSS analyses were performed by vacuum-filtering on 55 mm diameter glass fibre filters (Whatman GF/A, with a pore size of 1.6 μm) following the standardised method SS-EN 872:2005. The filters were pre-treated first in a muffle furnace (Carbolite furnaces CSF 12/13) at 500 °C for 30 minutes in aluminium cups, then filtrated with 150 ml of ultrapure water (Fisher Scientific Accu100 Ultrapure Water System) and dried for at least 1 h in an oven (Thermo Scientific Heratherm OGS60, 105 °C) and weighed. Due to the presence of non-water-soluble substances in some samples, the glass funnel was rinsed with ethanol and ultrapure water onto the filter, to avoid sample materials being left on the equipment. The filters were dried in the aluminium cups in the oven and were weighed after cooling in a desiccator. VSS (SS 02 81 13) was determined by burning the filters with the dried material in the aluminium cups for 2 hours in a furnace at 550 °C, followed by weighing after cooling in a desiccator. Information about analysed sample volumes and dry residuals on filters can be found in SI Table S12.

Turbidity was measured with a turbidimeter (WTW Turb 430-IR/T) 8–20 days after sampling. Measurements were performed by retrieving subsamples from the shaken bottles into a vial and measuring each subsample in triplicate. Standard solutions of 0.02, 10 and 1000 NTU were checked every day before beginning the analysis for calibration.

Samples from 2023-04-29 in GP2 were analysed for total metals 10–11 months after sampling. To ensure homogeneity and to dislodge possible material adhered on the glass bottles, samples were ultrasonicated and shaken. Subsamples of 30 mL were retrieved and sent for analysis of elements Na, K, Ca, Fe, Mn, Al, As, Ba, Pb, Cd, Co, Cu, Cr, Mo, Ni, V and Zn to a commercial lab using acid digestion and inductively coupled plasma mass spectrometry (ICP/MS) following the procedure in SS-EN ISO 17294-2:2016.

Statistical analysis

Statistical analyses were conducted in IBM SPSS Statistics 28 using median TWP concentrations (1.6–500 μm) from the Monte Carlo simulations. The normality of datasets was tested by Shapiro–Wilk normality tests. Spearman's rank order correlation tests were used to investigate the relationship between the TWP concentration and other measured parameters (SI 3.1.1). Multivariable linear regression analyses (OLS) were performed using the natural logarithm of TWP concentrations as the dependent variable, while the explanatory variables were time from the start of sampling (ratio variable ln-transformed) and sampling date (nominal variable; SI 3.1.2). Multivariable linear regression analysis was also used to explore the relationship between ln-transformed TWP concentrations and ln-transformed TSS for the rain event of 2023-04-29 (SI 3.1.3) and on the complete dataset of both rainfalls. The regression equation obtained from the 2023-04-29 data was used to predict TWP concentrations during the 2023-05-17 rain event based on the TSS data. Similarly, the regression equation obtained from the complete dataset of both rainfalls was used to estimate the TWP concentrations of the rain events from 2023-04-05, 2023-04-12 and 2023-04-23, based on TSS.

Results

The mean TWP concentrations from the Monte Carlo simulations are presented in the Results and the Discussion sections, whereas the SBR + BR concentrations and the distribution of TWP concentration in each sample can be found in SI Tables S9 and S10.

TWP concentrations in stormwater during rain events

The rain event on 2023-04-29 was of short duration (*ca.* 1 hour), with a high-intensity rain peak of 7 mm h^{-1} at 16:55 that triggered all three wells within 7 minutes (Fig. 2). The measured TWP concentrations (1.6–500 μm) during the time-series of the rain varied between 9.1 and 170 mg L^{-1} (Fig. 2). The wells, especially the gully pots GP1 and GP2, showed higher TWP concentrations at the beginning of the rain event. The observation that TWP concentrations decreased with rain duration was further evidenced by the negative correlation between the TWP concentration and time from the start of sampling ($r = -0.92$, Fig. 4).

On 2023-05-17, the automatic sampler in the gully pot GP2, the second well in the system, was triggered at 06:54 and again between 14:44 and 14:50 after which the sampler was full, whereas GP1 and WA were triggered in the latter part of the rainfall after 18:00 (Fig. 3). TWP concentrations (1.6–500 μm) varied between 10 and 80 mg L^{-1}, with concentrations decreasing over time ($r = -0.67$, Fig. 4), similarly to what was seen on 2023-04-29 even if less pronounced. The highest TWP concentrations were lower compared to the 2023-04-29 sampling. For both rainfalls, the flow data from the stormwater system, measured in the collecting well WA, were available. Based on the flow data and using the TWP concentrations in WA, the total mass load out from the stormwater system for the rain on 2023-04-29 was 204 g, with an event mean concentration (EMC) of 93 mg L^{-1}. Flow measurements in WA showed that 58% of TWP mass was emitted with the first 50% of the runoff volume. For the rain on 2023-05-17, 3.9 g of TWP was estimated to be emitted, with an EMC of 64 mg L^{-1}, and 47% of TWP mass was emitted with the first 46% of the runoff volume.

The results for both rainfalls show that a large proportion of TWP was in the fine fraction (1.6–20 μm): 47–100%, with an

 This journal is © The Royal Society of Chemistry 2025

Open Access Article. Published on 22 October 2025. Downloaded on 4/9/2026 1:40:24 PM.
This article is licensed under a Creative Commons Attribution 3.0 Unported Licence.

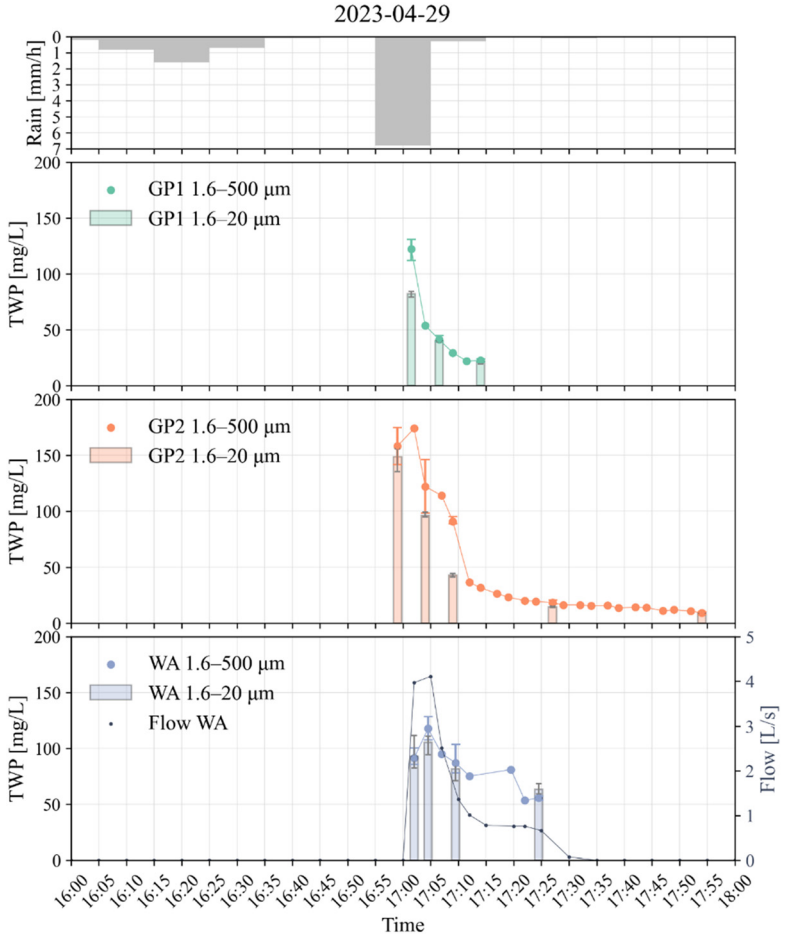

Fig. 2 Rain intensity measured every 10 minutes on 2023-04-29 and TWP concentrations in gully pots GP1 and GP2, and collecting well WA, together with the measured flow rate in WA over time. For samples analysed in replicates, average values are shown with error bars indicating minimum and maximum values.

average of 87 ± 13% (mean ± standard deviation). Linear regression showed that TWP concentrations were significantly decreasing with time from the start of the sampling (B = −0.4, SE = 0.06, $p < 0.001$), but the sampling date was not found to have a significant effect. The predicted TWP concentrations based on TSS for the rain events between 2023-04-05 and 2023-04-23 yielded values between 2.6 and 60 mg L^{-1} (SI Table S8), which are similar to the concentrations found from 2023-05-17.

Particulate materials and turbidity during rain events

TSS and VSS showed decreasing concentrations with time from the start of the sampling (SI 3.6). The analyses of VSS showed that organic materials ranged from 18 to 28% on 2023-04-29 with an average value of 21%, and slightly higher on 2023-05-17, ranging from 20 to 34% with an average of 24%. The turbidity values ranged from 38–378 NTU over both rain events, and were similar between the two rain events, on average 268 NTU on 2023-04-29 and 285 NTU on 2023-05-17 (SI 3.7). Turbidity did not show a decreasing trend with time from the start of sampling as clearly as the other parameters did, especially not on 2023-04-29. The ratio of TWP-to-TSS, measured on the 25 mm filter, was on average 6.3 ± 1.4% (mean and standard deviation), with slightly lower ratios of TWP-to-TSS on 2023-04-29, 5.8 ± 1.4%, compared to 2023-05-17, 7.2 ± 1.6%, SI Table S13.

For samples collected on 2023-04-29, the correlations between the TWP concentration, TSS and VSS were all very strong ($r > 0.9$, Fig. 4). The turbidity, however, only showed weak correlations with the TWP concentration (r = 0.17). The samples from 2023-05-17, Fig. 4, also showed very strong correlations between the TWP concentration, TSS and VSS (r = 0.9). The turbidity showed a strong correlation with the TWP concentration (r = 0.67) on 2023-05-17, which was not the case on 2023-04-29. The correlations on aggregated data for the two rain events can be found in SI Fig. S5. The linear regression equation obtained from the TWP and TSS concentrations on 2023-04-29 showed good prediction of the TWP concentrations on 2023-05-17 based on the measured TSS concentrations, with R^2 = 0.73 (SI 3.1.3).

Total metals in gully pot GP2 during the rain event on 2023-04-29

All total concentrations of the major elements Mg, Mn, Fe, K, Ca and Al, and the minor elements As, Ba, Cd, Co, Cr, Cu, Mo,

Open Access Article. Published on 22 October 2025. Downloaded on 4/9/2026 1:40:24 PM.
This article is licensed under a Creative Commons Attribution 3.0 Unported Licence.

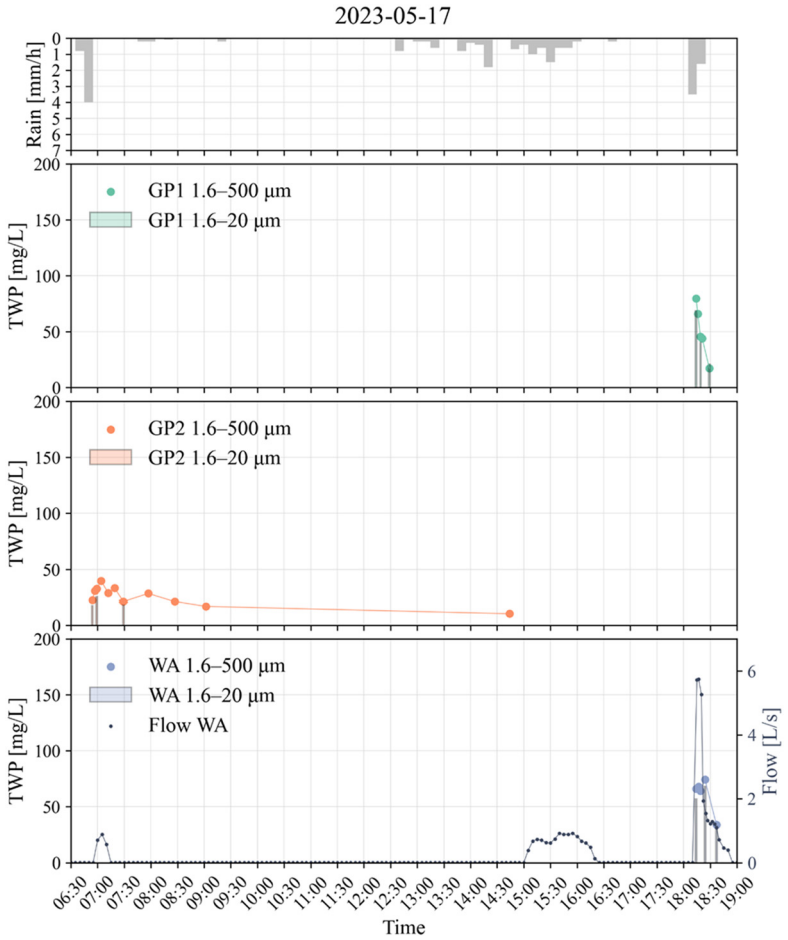

Fig. 3 Rain intensity measured every 10 minutes on 2023-05-17 and TWP concentrations in gully pots GP1 and GP2, and collecting well WA, together with the measured flow rate in WA over time.

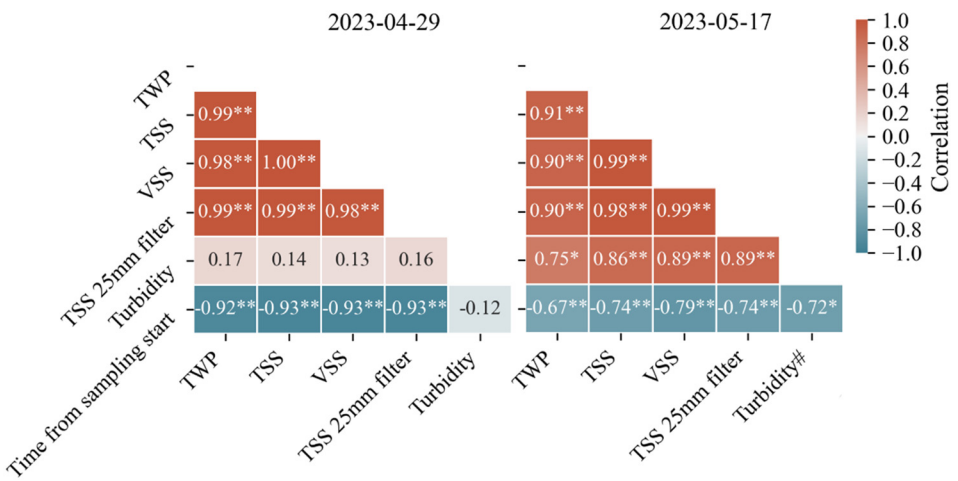

Fig. 4 Spearman's rank order correlation of the TWP concentration, VSS and TSS (using filter diameters of 55 mm and 25 mm), turbidity, and time in minutes from the start of the sampling. (Left) Correlation for 37 data points from all locations sampled on 2023-04-29. (Right) Correlation for 21 data points from all locations sampled on 2023-05-17, except for turbidity, for which 10 data points were measured, marked with #. (*) indicates that the correlation is significant at the 0.05 level. (**) indicates that the correlation is significant at the 0.01 level.

Ni, Pb, V and Zn, in gully pot GP2 varied strongly with time from the start of the sampling, with higher concentrations during the first intense peak of the rainfall, followed by a strong decrease, similarly to what was seen for TWP (Fig. 5). However,

 This journal is © The Royal Society of Chemistry 2025

Open Access Article. Published on 22 October 2025. Downloaded on 4/9/2026 1:40:24 PM.
This article is licensed under a Creative Commons Attribution 3.0 Unported Licence.

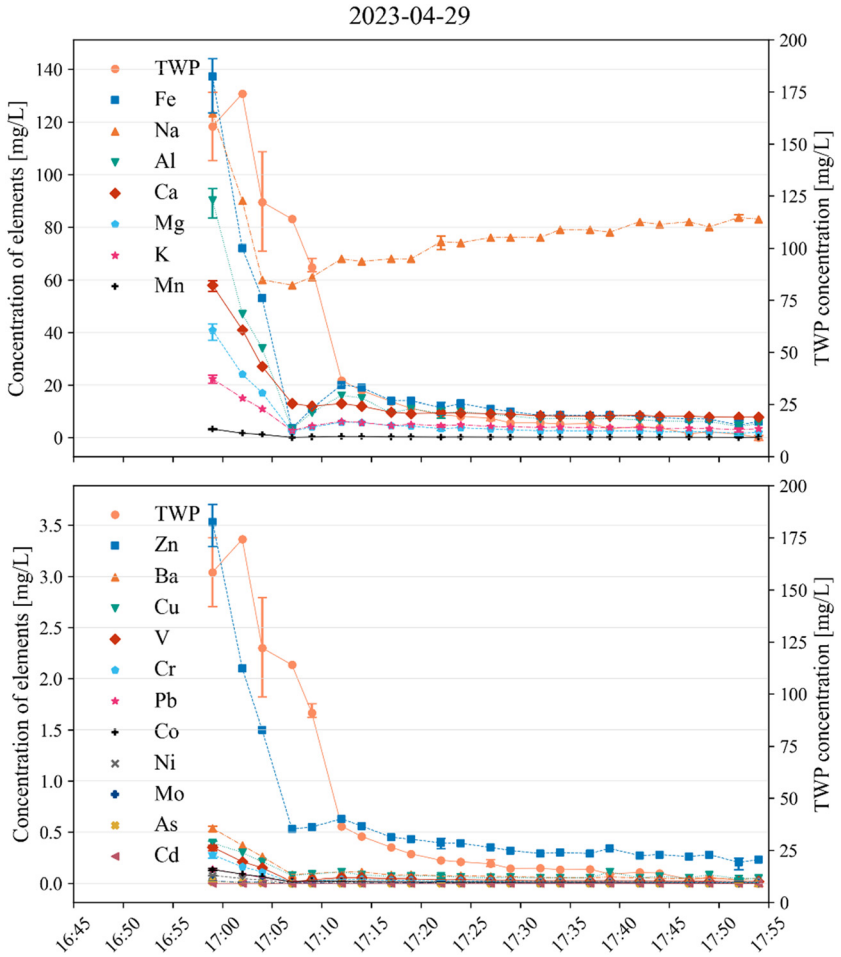

Fig. 5 Concentrations of elements and TWP in gully pot GP2 on 2023-04-29 with different axis limits for major and minor elements giving a better visualization between the top and bottom figures.

Na did not follow this pattern, showing more constant concentration during the rain event (Fig. 5). No elements, except for Ni, were quantified in a blank sample of ultrapure water.

The TWP concentration showed strong correlations ($r > 0.7$) with all elements, listed in order of decreasing strength as follows: Ca > Ba = Co > Zn > As > Pb > Mg > Ni > Mn > Mo > Al = Cr = Fe = V > Cu (Fig. 6). Correlations of TSS with elements were similar to correlations of the TWP concentration with elements. The correlation of the TWP concentration and TSS with Na was moderately negative ($r = -0.50$).

Discussion

TWP concentrations during rain: loads, proportion in the fine fraction of 1.6–20 μm, and ratio of TWP-to-TSS

The TWP concentrations measured in the gully pots and the well during rainfall (9.1–170 mg L^{-1}; Fig. 2 and 3) were much higher than previously reported values in the standing water of the wells of 0.52–2.9 mg L^{-1} found in grab samples of water from the same wells[17] analysed with the same Pyr-GC/MS technique as in the present study, and of 1.0 mg L^{-1} in well WA analysed with TED-GC/MS.[29] During rainfall, the TWP concentrations surpassed these values, reaching concentrations higher than those observed in tunnel wash water (15–48 mg L^{-1})[18] and runoff from a German highway with high AADT (51–59 mg L^{-1}).[29] These findings highlight the highly dynamic and transient behaviour of TWP concentrations during rain events. The elevated TWP concentrations during rain events suggest mobilisation from road surfaces *via* runoff or resuspension from sediments in the sand traps of the gully pots, as previous studies have shown that sediments in gully pots can contain substantial amounts of TWP,[17,18,38] which can be transported further downstream during rain. The high TWP concentrations observed in the last well WA of the studied stormwater system (Fig. 2 and 3) further indicate downstream transport. This aligns with findings from the same stormwater system, where TWP concentrations in sediments were shown to increase downstream.[17] The fine-sized TWP likely do not have time to settle in the small standing water volumes of the gully pots and the well under the dynamic and turbulent flow conditions during rain.

The mass load of TWP measured in well WA during the sampled rain events (see the TWP concentrations in stormwater

Open Access Article. Published on 22 October 2025. Downloaded on 4/9/2026 1:40:24 PM.
This article is licensed under a Creative Commons Attribution 3.0 Unported Licence.

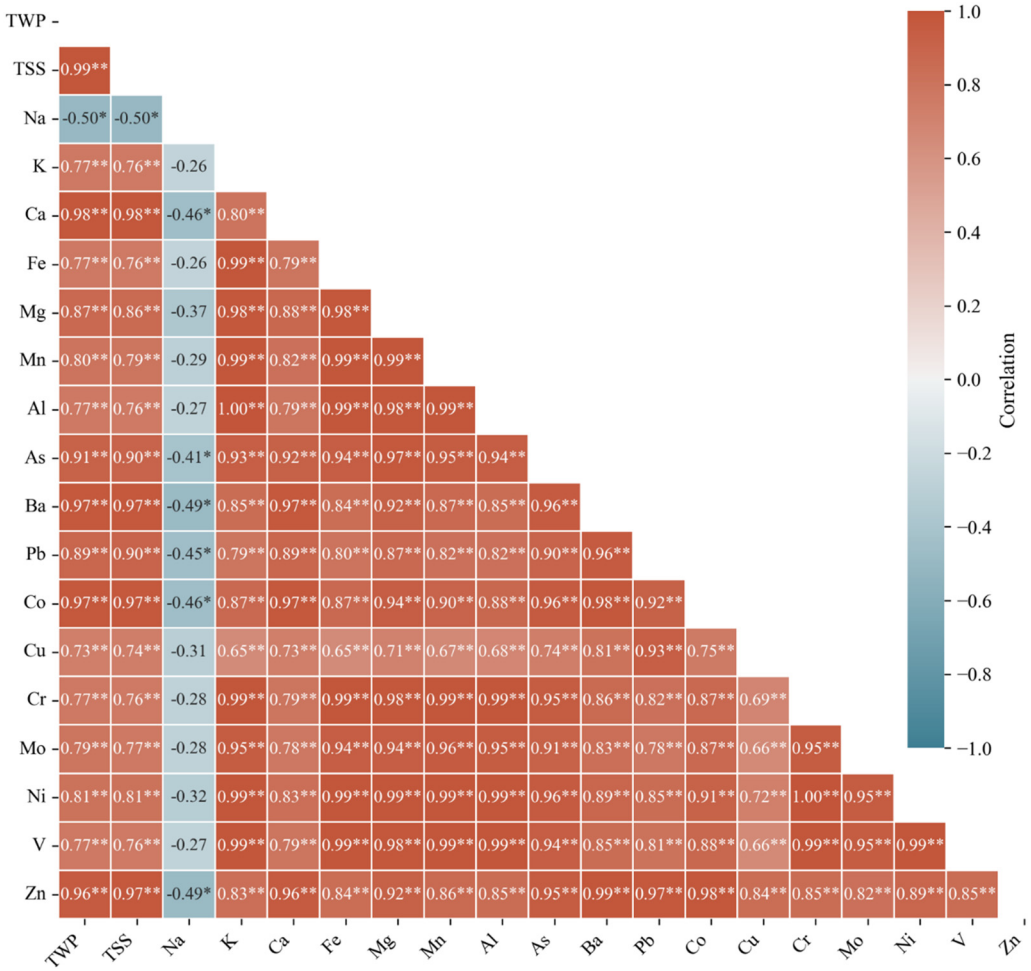

Fig. 6 Spearman's rank correlation matrix between TSS (measured on 25 mm filters), SBR + BR concentration, TWP concentration and element concentration for 2023-04-29 samples. (*) indicates that the correlation is significant at the 0.05 level (2-tailed). (**) indicates that the correlation is significant at the 0.01 level (2-tailed).

during rain events section) can be compared to the estimated TWP mass deposited on the road during the antecedent dry periods (see SI 1.2). On 2023-04-29, the TWP load in well WA, based on the measured concentration and flow rate, was 204 g, which is similar to the estimated 436 g of TWP deposited on the road surface at the onset of rain. This suggests that a large fraction of available TWP was mobilised and transported through the stormwater system. However, the resuspension of TWP previously sedimented in the wells may also have contributed to the measured TWP concentrations. For the 2023-05-17 rain event, the estimated mass of TWP available for mobilisation on the road was 116 g (SI 1.3), which was higher than the mass load of TWP in well WA (3.9 g). Part of this discrepancy may be explained by the lower rainfall intensity compared to the 2023-04-29 event, potentially reducing mobilisation efficiency. In addition, the delayed trigger of well WA on the 2023-05-17 rain likely affects the results: the sampler in well WA was not triggered until 18:00, 12 hours after the onset of the rain, therefore missing TWP previously transported through well WA by precipitation at 6:30 and 15:00 (Fig. 3).

The EMCs of TWP in the water of well WA (64–93 mg L^{-1}) exceeded those of other microplastics reported in stormwater from industrial and residential areas (0.035–0.78 mg L^{-1}, for particles >20 μm)[32] and in urban catchments (0.056 mg L^{-1}, for particles >80 μm).[33] Additionally, the high identified proportions of TWP in the fine fraction (1.6–20 μm; 47–100%) in the present study were similar to those found in stormwater from the standing water volumes of the same gully pots and wells, 60–93% with average 79%.[17] The proportion of TWP in the fine fraction was also higher than in snow from the same area, 46 ± 28%,[35] and in sediments from a German sedimentation basin with TWP mass for particles <20 μm between 20 and 40%.[39] The proportion of fine-sized TWP varied between samples, but no trend with respect to the rain event duration was found. This is in contrast with the behaviour of other microplastics, as Cho *et al.*[32] reported that the proportion of larger and heavier particles increased at the end of the rain events, but only particles >20 μm were analysed. The reason for this discrepancy could be that TWP and other microplastics exhibit different behaviour related to their morphology,

 This journal is © The Royal Society of Chemistry 2025

Open Access Article. Published on 22 October 2025. Downloaded on 4/9/2026 1:40:24 PM. This article is licensed under a Creative Commons Attribution 3.0 Unported Licence.

density and the size differences of the particles. Other potential reasons could be due to variations in rain characteristics or catchment topology, and the fact that most TWP are present in particle fractions <20 μm, making it difficult to assess the behaviour of larger sized TWP.

The ratios of TWP-to-TSS (6.3 ± 1.4%) were consistent between samples. Similar ratios of TWP-to-TSS have been reported by other studies. Two studies from the same location as the present study, the test site E18, reported 2–22% of TWP in road dust[40] and 0.07–7.8% of TWP-to-solids in snow.[35] From Norway, the ratio of TWP-to-TSS was reported to be 0.94–6.4% in tunnel road dust and 2.2–3.2% in tunnel wash water,[18] and 5.7% in roadside snow.[22] This indicates that the TWP-to-TSS ratios in this type of road environment are stable. More organic materials were found in the samples from 2023-05-17 from VSS analysis, compared to 2023-04-29 (SI Table S12), which is likely due to increasing biological activity with warmer spring temperatures, SI Fig. S1. The samples collected on 2023-05-17 more often yielded high concentrations of marker benzene, prompting the use of marker combination *b* for some samples (see SI Table S9).

Transport behaviour of TWP in the stormwater system based on correlations

The strong correlation between the TWP concentration and TSS/VSS (Fig. 4) indicates similar transport processes in stormwater during rainfall between TWP and particulate materials. Strong correlations between TWP and solids have been reported in other matrices as well, such as snow, stormwater samples and tunnel wash water[17,18,22,35] and also with organic matter in sediments.[41,42] Microplastics and suspended solids were found to also correlate very strongly ($r > 0.8$) in stormwater in industrial and residential catchments.[32] The regression analysis equation on the complete dataset (SI 3.1.3) could be used to predict TWP concentrations based on TSS concentrations, as they have shown good correlation, but further research is needed to assess that the relationship is not only site-specific or weather dependent.

The strong negative correlation with rain duration confirms the transient TWP concentrations in the system, elevated at the beginning of the rainfall due to mobilisation from the road or resuspension. Treilles *et al.*[33] similarly reported the highest MP concentrations just before the flow rate peak in a stormwater outlet, and that the concentrations were markedly lower at the end of the rainfall. However, this pattern was not observed for microplastics in stormwater from urban and suburban areas.[34] The difference in behaviour can be due to the different topologies of the area and rain or particle characteristics. The rain on 2023-04-29 presented higher concentrations at the beginning of the rain event, compared to the rain on 2023-05-17, likely due to the large intensity of the rain. Depending on which definition was used to define a first-flush, the outcomes for the sampled rains differ. Based on the definition of first-flush by Bertrand-Krajewski *et al.*,[43] a first-flush was not present in well WA neither on 2023-04-29 nor on 2023-05-17, as less than 80% of TWP mass was discharged with the first 30% of runoff volume. However, based on the dimensionless $M(V)$ curves (SI 3.5), the slope of the normalised cumulative mass emission *vs.* the normalised cumulative runoff volume was larger than 45° for the rain event on 2023-04-29, thus meeting the definition of first-flush by Geiger.[44] Given the limited number of rain events sampled, further monitoring across more events and locations is needed to determine whether TWP consistently exhibit first-flush behaviour.

The correlation between the TWP concentration and turbidity was not consistent between the rain events (Fig. 4). As turbidity measurements can be made remotely and automated, it is an important parameter for water quality monitoring.[45] Previous studies have found strong correlations between TSS and turbidity,[46,47] as well as between TSS and the TWP concentration,[17,18] suggesting that turbidity could serve as a proxy parameter for estimating TWP loads in stormwater from near-road environments. However, no correlation between turbidity and microplastic concentrations was observed in urban runoff.[48] Our results did also not show a predictable relationship between the TWP concentration and turbidity, but the results might be affected by the age of the samples when turbidity was analysed. Also, such a relationship is likely affected by multiple factors, such as the location and rain event characteristics and further studies are needed to assess whether turbidity can predict the TWP concentration in stormwater for certain systems.

Transient total metal behaviour during rainfall

All total elements measured showed peak concentrations at the beginning of the rainfall, which has also been observed for metals (and TSS) measured during seven rains.[49] Of the total metals measured, Na occurred in the highest concentration (Fig. 5), and it likely arises from residues of de-icing salt on the road and in the stormwater system, since it is a common winter maintenance practice in Sweden and on this highway section.[35] The different behaviour of Na and its weaker correlations with the TWP concentration and TSS compared to other metals were also seen in road-adjacent snow.[35] As metals and TSS also show a very strong correlation, this suggests that the high affinity between TWP and metals is due to similar transport patterns for particulate materials. In addition, the adherence/agglomeration of metals to TWP and subsequent co-transport cannot be excluded, as suggested by Gaggini *et al.*[35] and De Oliveira *et al.*[41] The average metal concentrations of Fe, Cd, Cr, Cu, Ni, and Zn were also higher than the average concentrations previously measured in road runoff,[49] but with similar Pb concentrations. As, Pb, Cd, Co, Cu, Cr, Ni, V, and Zn were higher than what was previously measured in runoff mostly originating from a highly trafficked highway in an urban area, sampled in sedimentation wells.[50]

Significance for stormwater management

TWP are one of the most important stormwater contaminants in near-road environments, and due to the negative effects of

Open Access Article. Published on 22 October 2025. Downloaded on 4/9/2026 1:40:24 PM. This article is licensed under a Creative Commons Attribution 3.0 Unported Licence.

the leachates of additives,[7–11] as well as the high estimated emissions, remediation actions are needed in sensitive areas with high traffic load. The findings in this study suggest that TWP are transported through the highway stormwater system during rain events. As 3545 tonnes per year are estimated to be emitted annually from highways in Sweden, with an additional 3333 tonnes per year from Swedish urban roads,[5] the TWP amounts transported through runoff from roads into sensitive recipients may be substantial. The relatively high TWP concentrations identified in the stormwater system during rain, together with previously detected TWP levels in the water and sediments of the recipient Lillån,[17] are an indication that environmental loads might be significant in certain receiving environments. To fully assess the environmental impact of TWP from stormwater systems, more information on the TWP loads into recipients is needed.

The design of the gully pots on Testsite E18 is of the same type as that often found in Sweden. Based on the concentrations identified in this study, the gully pots were found not to retain TWP during rain, as was suggested by TWP concentrations in sediments from the same stormwater system.[17] The strong correlations between the TWP concentration and TSS, VSS and total metals indicate that these parameters likely have similar transport patterns in the particulate form. Due to the prevalence of fine-sized (1.6–20 μm) TWP, traditional sedimentation-based measures are not likely to be effective, unless very long settling times are ensured.[51] Promising results for TWP remediation have been reported for stormwater treatment solutions such as raingardens, porous asphalt, stormwater ponds and infiltration ponds,[25,50,52–54] which should be further assessed. Moreover, stormwater solutions targeting TWP in this type of road environment should also target the high concentrations of metals, especially Cr, Cu and Zn, as well as dissolved metal fractions to avoid leaching.[49]

The elevated TWP concentrations at the beginning of the rainfall may indicate a first-flush effect, where peak flows mobilise TWP. However, the high concentrations may also result from resuspension of sediments in the wells due to turbulence. Regardless, the concentrations emitted from the stormwater system are high, and the TWP behaviour in the stormwater system is dynamic, highlighting the need for stormwater solutions to address this variability. This knowledge can help assess whether regular maintenance, such as sand trap emptying, or stormwater system designs preventing resuspension could be effective measures to limit high TWP emissions during rain. Also, the findings from the study can provide novel inputs to hydrological and hydrodynamic models describing TWP transport,[55,56] which in turn can be useful tools for the prioritisation of mitigation measures.

Limitations and recommendations for future research

The study addresses a significant knowledge gap regarding the occurrence and temporal variability of TWP in stormwater during rain events. There are several challenges and limitations that still need to be addressed in the sampling and analysis of TWP in stormwater facilities, warranting further investigations. Only a limited number of rainfall events could be sampled due to weather conditions and time constraints, which limits the extent to which the observed statistical results and trends can be applied more broadly. While the results show decreasing TWP concentrations in the stormwater with rain duration, definitive first-flush effects could not be confirmed. Future studies should include more rain events with different characteristics and other locations to assess how TWP concentrations in runoff are affected by rain dynamics and properties, such as antecedent dry days, rain duration and rain intensity, seasonality and the catchment type.

The quantification of TWP in environmental samples still poses many analytical challenges, including the variability in tyre formulations,[14] with appropriate methods and analytical markers still under development. In this study, the uncertainty stemming from the variation of SBR + BR content across different tyre types was estimated through the Monte Carlo approach by providing a distribution of TWP concentrations based on reference tyres (SI 3.3), as done in some previous studies.[15,17,18,21,22,35] This variation in SBR + BR content across different tyres needs to be considered when evaluating the results. Additional uncertainties in the analytical results for certain parameters may arise from the extended storage time of the samples, which were kept consistently refrigerated and in the dark to minimise sample degradation. For the TSS parameter, previous studies have suggested that the results should not be affected considerably by the storage time.[17,57] The storage in glass bottles was preferred to avoid contamination from plastic materials in the TWP analyses, but the storage may have caused adsorption of elements on the container walls.[58,59] To minimise underestimation of the total metal concentrations, the ultrasonication step was added before metal analysis to release particles that were possibly attached to the container walls during storage.

The gully pots of the studied highway stormwater system were found not to retain TWP for the studied rain events, based on the high concentrations throughout the system. The trapping efficiencies of stormwater systems for TWP could be assessed in more detail by future studies, to yield a deeper understanding of the specific mechanisms affecting efficiency, such as the effect of different designs, flow rates and particle sizes, which have been investigated for microplastics and particulate materials.[60–63] Also, further research is needed to separately assess the mobilisation of TWP from road surfaces during rain events, and the extent of resuspension from sediments in stormwater systems. Furthermore, the study was conducted on a single stormwater system, and more research is needed to assess whether the findings are site-specific or have broader applicability.

Conclusions

This study demonstrates the abundance and dynamic behaviour of tyre wear particles (TWP) in stormwater during rain events:

 This journal is © The Royal Society of Chemistry 2025

Open Access Article. Published on 22 October 2025. Downloaded on 4/9/2026 1:40:24 PM.
This article is licensed under a Creative Commons Attribution 3.0 Unported Licence.

• The high TWP concentrations (89–170 mg L^{-1}) measured throughout the stormwater system highlight the high transport potential of TWP, particularly for the fine fraction (1.6–20 μm), which was found to be more abundant than the larger size fraction (20–500 μm).

• The high concentrations of TWP and metals at the onset of rain suggest first-flush effects or sediment resuspension, underscoring the need for management strategies that address these dynamic processes.

• Strong correlations between the TWP concentration, suspended solids (TSS, VSS), and total metals indicate shared transport pathways in stormwater systems during rain events.

• In addition to TWP, high concentrations of metals, such as Cr, Cu, and Zn, were identified.

The high TWP concentrations observed in this study underline the need to address TWP as a pollutant of concern in near-road environments, and greater knowledge of TWP loads reaching sensitive recipients is required to assess environmental impacts. The findings highlight key processes, such as elevated concentrations during wet-weather events throughout a stormwater system, dynamic transport behaviour, and the predominance of fine-sized TWP. These features may limit the effectiveness of traditional sedimentation-based measures and should be considered when designing management strategies. Future studies should investigate a wider range of rain events and locations to assess how rainfall dynamics and catchment characteristics influence TWP concentrations in runoff. In addition, more research is needed to quantify the transport of TWP to receiving waters and to evaluate the effectiveness of different treatment solutions.

Author contributions

Elly Lucia Gaggini: conceptualization, formal analysis, funding acquisition, investigation, methodology, validation, visualization, writing – original draft, writing – review & editing. Ekaterina Sokolova: conceptualization, funding acquisition, methodology, project administration, supervision, writing – review & editing. Elisabeth Støhle Rødland: formal analysis, investigation, methodology, writing – review & editing. Ann-Margret Strömvall: methodology, writing – review & editing. Yvonne Andersson-Sköld: conceptualization, methodology, supervision, writing – review & editing. Mia Bondelind: conceptualization, funding acquisition, methodology, project administration, supervision, writing – review & editing.

Conflicts of interest

There are no conflicts to declare.

Data availability

The data supporting this article have been included as part of the supplementary information (SI).

Supplementary information is available. See DOI: **https://doi.org/10.1039/d5ew00656b**.

Acknowledgements

This work was supported by the Swedish Research Council (FORMAS) [2019-00284], the Norwegian Public Road Administration [B11191 Ferjefri E39], the J. Gustaf Richert Foundation [2022-00807], the Sveriges Ingenjörer Environmental Fund [2022], the Adlerbertska Research Foundation [2022], and the Åke and Greta Lissheds Foundation [2022-00188]. The authors are grateful to: the Swedish Road Administration for support on Testsite E18 and for providing weather and traffic data, Alberto Celma for assistance with sample retrieval, Amir Saeid Mohammadi for helping with the laboratory work, and Niels Markwat for assistance with statistical analysis of the data.

References

1 H. Österlund, G. Blecken, K. Lange, J. Marsalek, K. Gopinath and M. Viklander, *Sci. Total Environ.*, 2023, **858**, 159781, DOI: **10.1016/j.scitotenv.2022.159781**.

2 M. U. Ali, S. Lin, B. Yousaf, Q. Abbas, M. Ahmed, M. Munir, M. U. Ali, A. Rasihd, C. Zheng, X. Kuang and M. H. Wong, *Sci. Total Environ.*, 2021, **791**, 148422, DOI: **10.1016/j.scitotenv.2021.148422**.

3 N. B. Hartmann, T. Hüffer, R. C. Thompson, M. Hassellöv, A. Verschoor, A. E. Daugaard, S. Rist, T. Karlsson, N. Brennholt, M. Cole, M. P. Herrling, M. C. Hess, N. P. Ivleva, A. L. Lusher and M. Wagner, *Environ. Sci. Technol.*, 2019, **53**, 1039–1047, DOI: **10.1021/acs.est.8b05297**.

4 P. J. Kole, A. J. Löhr, F. G. A. J. Van Belleghem and A. M. J. Ragas, *Int. J. Environ. Res. Public Health*, 2017, **14**(10), DOI: **10.3390/ijerph14101265**.

5 M. Polukarova, M. Hjort and M. Gustafsson, *Sci. Total Environ.*, 2024, **924**, 171391, DOI: **10.1016/j.scitotenv.2024.171391**.

6 D. Mennekes and B. Nowack, *Sci. Total Environ.*, 2022, **830**, 154655, DOI: **10.1016/j.scitotenv.2022.154655**.

7 Z. Tian, H. Zhao, K. T. Peter, M. Gonzalez, J. Wetzel, C. Wu, X. Hu, J. Prat, E. Mudrock, R. Hettinger, A. E. Cortina, R. G. Biswas, F. V. C. Kock, R. Soong, A. Jenne, B. Du, F. Hou, H. He, R. Lundeen, A. Gilbreath, R. Sutton, N. L. Scholz, J. W. Davis, M. C. Dodd, A. Simpson, J. K. McIntyre and E. P. Kolodziej, *Science*, 2021, **371**, 185–189, DOI: **10.1126/science.abd6951**.

8 A. Wik and G. Dave, *Chemosphere*, 2006, **64**, 1777–1784, DOI: **10.1016/j.chemosphere.2005.12.045**.

9 T. S. Page, R. Almeda, M. Koski, E. Bournaka and T. G. Nielsen, *Aquat. Toxicol.*, 2022, **252**, 106299, DOI: **10.1016/j.aquatox.2022.106299**.

10 L. Chen, Z. Liu, T. Yang, W. Zhao, Y. Yao, P. Liu and H. Jia, *Environ. Sci. Technol.*, 2023, **58**(10), DOI: **10.1021/acs.est.3c07878**.

11 P. Boisseaux, C. Rauert, P. Dewapriya, M. L. Delignette-Muller, R. Barrett, L. Durndell, F. Pohl, R. Thompson, K. V. Thomas and T. Galloway, *J. Hazard. Mater.*, 2024, **466**, 133580, DOI: **10.1016/j.jhazmat.2024.133580**.

Open Access Article. Published on 22 October 2025. Downloaded on 4/9/2026 1:40:24 PM. This article is licensed under a Creative Commons Attribution 3.0 Unported Licence.

12 E. S. Rødland, G. Binda, D. Spanu, S. Carnati, L. R. Bjerke and L. Nizzetto, *J. Hazard. Mater.*, 2024, **476**, 135042, DOI: **10.1016/j.jhazmat.2024.135042**.
13 E. S. Rødland, M. Gustafsson, D. Jaramillo-Vogel, I. Järlskog, K. Müller, C. Rauert, J. Rausch and S. Wagner, *TrAC, Trends Anal. Chem.*, 2023, **165**, 117121, DOI: **10.1016/j.trac.2023.117121**.
14 Y. Ma, X. Chen, J. Li, E. S. Rødland and Y. Lin, *Environ. Sci. Technol.*, 2025, **59**(25), DOI: **10.1021/acs.est.4c12492**.
15 E. S. Rødland, L. S. Heier, O. C. Lind and S. Meland, *Sci. Total Environ.*, 2023, **903**, 166470, DOI: **10.1016/j.scitotenv.2023.166470**.
16 C. Rauert, E. S. Rødland, E. D. Okoffo, M. J. Reid, S. Meland and K. V. Thomas, *Environ. Sci. Technol. Lett.*, 2021, **8**, 231–236, DOI: **10.1021/acs.estlett.0c00949**.
17 E. L. Gaggini, M. Polukarova, M. Bondelind, E. S. Rødland, A.-M. Strömvall, Y. Andersson-Sköld and E. Sokolova, *J. Environ. Manage.*, 2024, **367**, 121989, DOI: **10.1016/j.jenvman.2024.121989**.
18 E. S. Rødland, O. C. Lind, M. Reid, L. S. Heier, E. Skogsberg, B. Snilsberg, D. Gryteselv and S. Meland, *J. Hazard. Mater.*, 2022, **435**, 129032, DOI: **10.1016/j.jhazmat.2022.129032**.
19 E. S. Rødland, S. Samanipour, C. Rauert, E. D. Okoffo, M. J. Reid, L. S. Heier, O. C. Lind, K. V. Thomas and S. Meland, *J. Hazard. Mater.*, 2022, **423**(Part A), 127092, DOI: **10.1016/j.jhazmat.2021.127092**.
20 S. Meland, G. M. Granheim, J. T. Rundberget and E. Rødland, *Environ. Sci. Technol. Lett.*, 2024, **11**, 35–40, DOI: **10.1021/acs.estlett.3c00811**.
21 M. Polukarova, E. L. Gaggini, E. S. Rødland, E. Sokolova, M. Bondelind, M. Gustafsson, A.-M. Strömvall and Y. Andersson-Sköld, *Environ. Pollut.*, 2025, **372**, 125971, DOI: **10.1016/j.envpol.2025.125971**.
22 E. S. Rødland, O. C. Lind, M. J. Reid, L. S. Heier, E. D. Okoffo, C. Rauert, K. V. Thomas and S. Meland, *Sci. Total Environ.*, 2022, **824**, 153785, DOI: **10.1016/j.scitotenv.2022.153785**.
23 T. R. Barber, F. Ribeiro, S. Claes, Y. Kawamura, J. Yeung, H. A. Byrne, S. Weyrauch, T. Reemtsma and K. M. Unice, *Mar. Pollut. Bull.*, 2025, **211**, 117363, DOI: **10.1016/j.marpolbul.2024.117363**.
24 T. R. Barber, S. Claes, F. Ribeiro, A. E. Dillon, S. L. More, S. Thornton, K. M. Unice, S. Weyrauch and T. Reemtsma, *Sci. Total Environ.*, 2024, **913**, 169633, DOI: **10.1016/j.scitotenv.2023.169633**.
25 L. A. Rasmussen, F. Liu, N. D. R. Klemmensen, J. Lykkemark and J. Vollertsen, *Water Res.*, 2024, **248**, 120835, DOI: **10.1016/j.watres.2023.120835**.
26 I. Goßmann, M. Halbach and B. M. Scholz-Böttcher, *Sci. Total Environ.*, 2021, **773**, 145667, DOI: **10.1016/j.scitotenv.2021.145667**.
27 B. Rosso, E. Gregoris, L. Litti, F. Zorzi, M. Fiorini, B. Bravo, C. Barbante, A. Gambaro and F. Corami, *Environ. Pollut.*, 2023, **326**, 121511, DOI: **10.1016/j.envpol.2023.121511**.
28 R. Chand, I. Putna-Nīmane, E. Vecmane, J. Lykkemark, J. Dencker, A. Haaning Nielsen, J. Vollertsen and F. Liu, *Environ. Int.*, 2024, **188**, 108782, DOI: **10.1016/j.envint.2024.108782**.
29 R. Dröge and P. Tromp, CEDR Call 2016: Environmentally Sustainable Roads: Surface-and Groundwater Quality, 2019.
30 S. Ziajahromi, D. Drapper, A. Hornbuckle, L. Rintoul and F. D. L. Leusch, *Sci. Total Environ.*, 2020, **713**, 136356, DOI: **10.1016/j.scitotenv.2019.136356**.
31 K. Lange, K. Magnusson, M. Viklander and G.-T. Blecken, *Water Res.*, 2021, **202**, 117457, DOI: **10.1016/j.watres.2021.117457**.
32 Y. Cho, W. J. Shim, S. Y. Ha, G. M. Han, M. Jang, S. H. Hong, J. Shim, S. Y. Ha, M. Han, M. Jang and S. H. Hong, *Sci. Total Environ.*, 2023, **866**, 161318, DOI: **10.1016/j.scitotenv.2022.161318**.
33 R. Treilles, J. Gasperi, A. Gallard, M. Saad, R. Dris, C. Partibane, J. Breton and B. Tassin, *Environ. Pollut.*, 2021, **287**, 117352, DOI: **10.1016/j.envpol.2021.117352**.
34 L. Ochoa, J. Chan, C. Auguste, G. Arbuckle-Keil and N. L. Fahrenfeld, *Sci. Total Environ.*, 2024, **929**, 172485, DOI: **10.1016/j.scitotenv.2024.172485**.
35 E. L. Gaggini, E. Sokolova, E. S. Rødland, A.-M. Strömvall, Y. Andersson-Sköld and M. Bondelind, *Environ. Challenges*, 2025, **20**, 101228, DOI: **10.1016/j.envc.2025.101228**.
36 Swedish Transport Administration, Testsite E18 – a road research station, **https://www.trafikverket.se/resa-och-trafik/forskning-och-innovation/aktuell-forskning/transport-pa-vag/testsite-e18–en-vagforskningsstation/**, (accessed 4 October, 2021).
37 Swedish Transport Administration, NVDB on map, **https://nvdbpakarta.trafikverket.se/map**, (accessed 5 April, 2024).
38 D. Mengistu, A. Heistad and C. Coutris, *Sci. Total Environ.*, 2021, **769**, 144785, DOI: **10.1016/j.scitotenv.2020.144785**.
39 P. Klöckner, B. Seiwert, P. Eisentraut, U. Braun, T. Reemtsma and S. Wagner, *Water Res.*, 2020, **185**, 116262, DOI: **10.1016/j.watres.2020.116262**.
40 I. Järlskog, D. Jaramillo-Vogel, J. Rausch, M. Gustafsson, A. M. Strömvall and Y. Andersson-Sköld, *Environ. Int.*, 2022, **170**, 107618, DOI: **10.1016/j.envint.2022.107618**.
41 T. De Oliveira, D. P. T. Dang, M. Chaillou, S. Roy, N. Caubrière, M. Guillon, D. Mabilais, S. Ricordel, L. Jean-Soro, B. Béchet, B. M. Paslaru, L. Poirier and J. Gasperi, *Sci. Total Environ.*, 2024, **955**, 176855, DOI: **10.1016/j.scitotenv.2024.176855**.
42 K. M. Unice, M. L. Kreider and J. M. Panko, *Environ. Sci. Technol.*, 2013, **47**, 8138–8147, DOI: **10.1021/es400871j**.
43 J.-L. Bertrand-Krajewski, G. Chebbo and A. Saget, *Water Res.*, 1998, **32**, 2341–2356, DOI: **10.1016/S0043-1354(97)00420-X**.
44 W. Geiger, in *Proceedings of the 4th International Conference Urban Drainage*, Lausanne, 1987, pp. 40–46.
45 L. Parra, J. Rocher, J. Escrivá and J. Lloret, *Aquac. Eng.*, 2018, **81**, 10–18, DOI: **10.1016/j.aquaeng.2018.01.004**.
46 H. Rügner, M. Schwientek, B. Beckingham, B. Kuch and P. Grathwohl, *Environ. Earth Sci.*, 2013, **69**, 373–380, DOI: **10.1007/s12665-013-2307-1**.
47 S. Al Ali, C. Bonhomme and G. Chebbo, *Water*, 2016, **8**(8), DOI: **10.3390/w8080312**.
48 S. Lindfors, H. Österlund, C. Lorenz, A. Vianello, K. Nordqvist, K. Gopinath, J. Lykkemark, L. Lundy, J. Vollertsen

 This journal is © The Royal Society of Chemistry 2025

Open Access Article. Published on 22 October 2025. Downloaded on 4/9/2026 1:40:24 PM.
This article is licensed under a Creative Commons Attribution 3.0 Unported Licence.

and M. Viklander, *Sci. Total Environ.*, 2025, **980**, 179527, DOI: **10.1016/j.scitotenv.2025.179527**.

49 M. Boller, S. Langbein and M. Steiner, in *Highway and Urban Environment: Proceedings of the 8th Highway and Urban Environment Symposium*, ed. G. M. Morrison and S. Rauch, Springer, 2007, pp. 441–452.

50 G. Johansson, K. K. Fedje, O. Modin, M. Haeger-Eugensson, W. Uhl, Y. Andersson-Sköld and A. M. Strömvall, *J. Hazard. Mater.*, 2024, **468**, 133532, DOI: **10.1016/j.jhazmat.2024.133532**.

51 C. Vogelsang, A. L. Lusher, M. E. Dadkhah, I. Sundvor, M. Umar, S. B. Ranneklev, D. Eidsvoll and S. Meland, Microplastics in road dust – characteristics, pathways and measures REPORT SNO. 7526-2020, 2020.

52 C. J. Mitchell and A. D. Jayakaran, *Sci. Total Environ.*, 2024, **908**, 168236, DOI: **10.1016/j.scitotenv.2023.168236**.

53 L. A. Rasmussen, J. Lykkemark, T. Raaschou Andersen and J. Vollertsen, *Sci. Total Environ.*, 2023, **869**, 161770, DOI: **10.1016/j.scitotenv.2023.161770**.

54 P. N. Carvalho, O. Stein, E. Lauchnor, L. Johnson, M. Martens, A. Rizzo, R. Bresciani, F. Masi, C. Sarti, J. Pueyo, E. Mendoza, M. Riva, E. Rødland, S. Karlstrøm, A. Gragne, P. Molle, M. C. Lippera and J. Friesen, Monitoring Final Report. MULTISOURCE Deliverable 1.2, 2024.

55 M. Bondelind, E. Sokolova, A. Nguyen, D. Karlsson, A. Karlsson and K. Björklund, *Environ. Sci. Pollut. Res.*, 2020, **27**, 24218–24230, DOI: **10.1007/s11356-020-08637-z**.

56 K. M. Unice, M. P. Weeber, M. M. Abramson, R. C. D. Reid, J. A. G. Van Gils, A. A. Markus, A. D. Vethaak and J. M. Panko, *Sci. Total Environ.*, 2019, **646**, 1639–1649, DOI: **10.1016/j.scitotenv.2018.07.368**.

57 F. W. Oudyn, D. J. Lyons and M. J. Pringle, *Water Sci. Technol.*, 2012, **66**, 1310–1316, DOI: **10.2166/wst.2012.316**.

58 G. E. Batley and D. Gardner, *Water Res.*, 1977, **11**, 745–752, DOI: **10.1016/0043-1354(77)90042-2**.

59 A. L. R. Sekaly, C. L. Chakrabarti, M. H. Back, D. C. Grégoire, J. Y. Lu and W. H. Schroeder, *Anal. Chim. Acta*, 1999, **402**, 223–231, DOI: **10.1016/S0003-2670(99)00529-2**.

60 B. Stride, C. Dykes, S. Abolfathi, M. Jimoh, G. D. Bending and J. Pearson, *Sci. Total Environ.*, 2023, **899**, 165683, DOI: **10.1016/j.scitotenv.2023.165683**.

61 A. K. Howard, O. Mohseni, M. Asce, J. S. Gulliver, F. Asce and H. G. Stefan, *J. Hydraul. Eng.*, 2012, **138**(6), DOI: **10.1061/(ASCE)HY.1943-7900.0000544**.

62 A. Ciccarello, A. Bolognesi, M. Maglionico and S. Artina, *Water Sci. Technol.*, 2012, **65**, 15–21, DOI: **10.2166/wst.2011.775**.

63 M. Rietveld, F. Clemens and J. Langeveld, *Urban Water J.*, 2020, **17**, 669–680, DOI: **10.1080/1573062X.2020.1823430**.